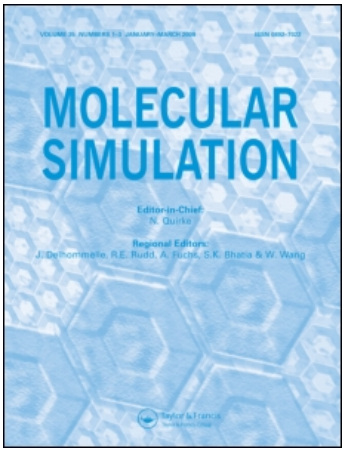

Molecular Simulation
Publication details, including instructions for authors and subscription information:
http://www.informaworld.com/smpp/title~content=t713644482

Determination of Structural Features in Simulated Amorphous Materials by Straightforward Methods

Luis Guillermo Cota[a]; Gerardo Vega[a]; Rodrigo Correa[a]; Luis Javier Alvarez[a]
[a] Laboratorio de Simulación de Materiales, Dirección General de Servicios de Cómputo Académico, Universidad Nacional Autónoma de México, Mexico, D. F., Mexico

To cite this Article Cota, Luis Guillermo , Vega, Gerardo , Correa, Rodrigo and Alvarez, Luis Javier(1998) 'Determination of Structural Features in Simulated Amorphous Materials by Straightforward Methods', Molecular Simulation, 20: 5, 315 — 330
To link to this Article: DOI: 10.1080/08927029808022040
URL: http://dx.doi.org/10.1080/08927029808022040

Molecular Simulation, 1998, Vol. 20, pp. 315–330
Reprints available directly from the publisher
Photocopying permitted by license only

DETERMINATION OF STRUCTURAL FEATURES IN SIMULATED AMORPHOUS MATERIALS BY STRAIGHTFORWARD METHODS

LUIS GUILLERMO COTA, GERARDO VEGA, RODRIGO CORREA and LUIS JAVIER ALVAREZ†

Laboratorio de Simulación de Materiales, Dirección General de Servicios de Cómputo Académico, Universidad Nacional Autónoma de México, Insurgentes Sur 3000, Zona Cultural, Ciudad Universitaria, Coyoacán 04510, Mexico, D. F., Mexico

(Received July 1997)

We present a variant of the "Swiss-cheese" model to allocate the maximum void volume in a simulated structure while minimizing the number of holes. The algorithm performance is not dependent upon user-adjustable parameters and there are no restrictions as to the type of target structure. A procedure to analyse connectivity in a structure, according to a criterion established here, is also presented. An alternate form of a percolation graph is suggested. The algorithms were tested on a simulated vitreous silica matrix, obtained by charge-transfer molecular dynamics. The results obtained in agreement with theoretical and experimental values regarding the percolation and gas-solubility behaviour of this structure.

Keywords: Free volume; charge-transfer molecular dynamics; gas solubility; percolation; silicon dioxide; silica

1. INTRODUCTION

In a simulated system it is often necessary to locate spatial positions where the structure is not as tightly packed as elsewhere and thus an atomic probe, or "penetrant" of a given size can be inserted. This insertion has its counterpart in physical processes such as ionic and gas diffusion, adsorption

†Corresponding author.

and catalysis, to name a few, where the size of the dissolving chemical species plays a decisive role.

The spatial distribution of such void positions can be seen as a complementary structure, and it can provide a useful alternative description of the system. This is specially relevant when dealing with amorphous systems, where the absence of long-range periodicity adds further complications to the structural description.

In the past a good amount of effort has been invested in describing in various ways the peculiarities of cavity systems, either departing from a dense random packed array of hard spheres [1, 2, 3, 4, 5, 6] or from a simulated molecular conglomerate [7, 11, 12, 13, 15, 16]. Cavity structure is described in several ways, among them the analysis of polyhedra that confine patches of free space [1, 2, 3, 4, 5, 6, 16], grid analysis [13], local conformation analysis [7] and random position generation procedures (more quaintly known as "Swiss-cheese" models) [15]. Takeuchi [12], Sok and Berendsen [13] and Greenfield and Theodorou [16] analysed the time evolution of cavities in polymeric materials.

In terms of programming and computational time, probabilistic models outperform most deterministic algorithms and are capable of producing useful and accurate information, as we shall see below.

2. MOLECULAR DYNAMICS SIMULATION

2.1. Charge-Transfer Molecular Dynamics

In order to properly model the partly covalent nature of the silica structure we resorted to an empirical scheme developed by Alavi *et al.* [8]. In this approach charge, as a function of distance, is influenced by the local environment and is calculated at every time step during the simulation. It is thus possible to follow the time evolution of the charge of a given atom and determine its structural role on electrical as well as on positional grounds.

2.2. Sample Preparation Procedure

The starting point of our simulation was a pure amorphous SiO_2 configuration consisting of 648 particles (216 silicon and 432 oxygen atoms) originally used in [8], subjected to periodic boundary conditions to simulate an infinite solid. The density of our pure SiO_2 glass sample was the commonly reported value of 2.2 g/cm^3, which corresponds to a cubic computational cell of 21.4003 Å.

The molecular dynamics run was carried out in two phases: a primary phase consisting of 5,000 time steps (5 ps), was carried out in which the particle velocities were artificially rescaled to represent, on average, the desired temperature. In the next phase, the temperature constraint was relaxed, and the system was left to evolve freely. After 15,000 time steps (15 ps) and the temperature had not deviated more than 4% from the initially set value, 300 K, and the sample was considered stable and ready for further analysis. Our simulated system is represented in Figure 1.

A common way of characterising an amorphous material is through its radial distribution function, RDF, obtained from diffraction experiments. The RDF reflects the material's characteristic interatomic distances. Figure 2 shows the RDF of the simulated amorphous silica shown in Figure 1.

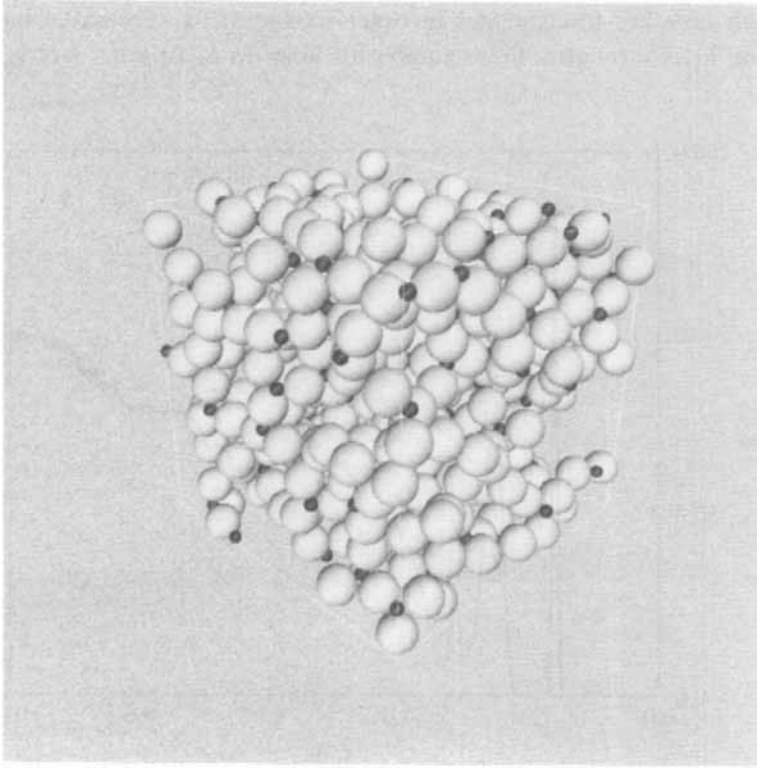

FIGURE 1 Original amorphous SiO_2 structure was originally from [8], after a 20,000-step charge-transfer molecular dynamics run. It contains 216 SiO_2 units (648 particles in total). All other figures refer to this structure, unless otherwise noted. Its corresponding cavity structure is shown in Figure 4. (See Color Plate I).

There is complete agreement with the classical experimental values reported by Mozzi and Warren [9].

3. CAVITY ANALYSIS

3.1. Algorithm Description

A simple way of describing void space between atoms, V_{void}, within a box of volume V, is by a set, S, of spheres, that we call "holes", which are totally contained in V_{void}. The set S has to comply with two properties, namely that the total volume of the holes, V_{holes}, is approximately equal to V_{void} (and thus $V \approx V_p + V_{holes}$, where V_p is the total volume of the particles contained in the box), and that the cardinality (the number of elements) of the set is not excessively large. Consequently, the right choice of size and the location of each hole are fundamental in order to allocate a substantial part of volume V_{void} through a finite number of holes in S. In other words, it is

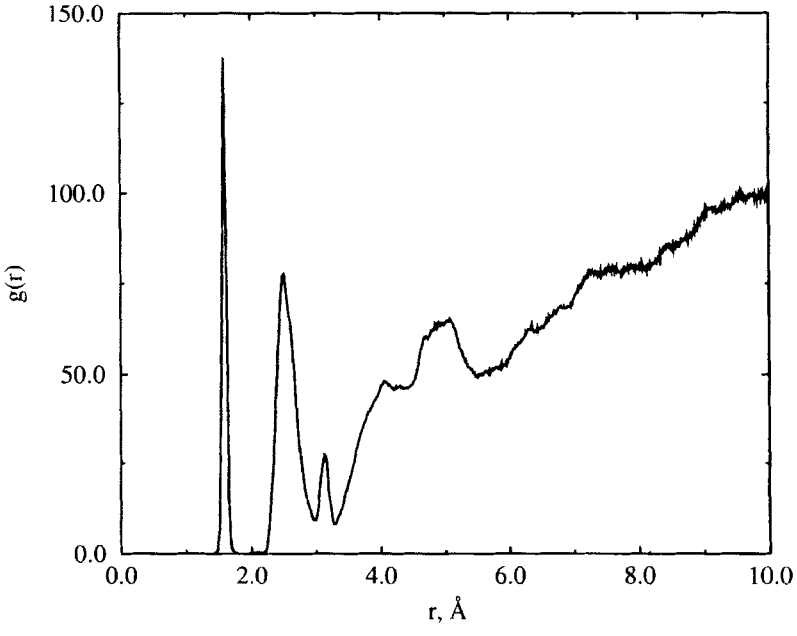

FIGURE 2 Total radial distribution function for the amorphous silica structure of Figure 1. The peaks shown correspond to the typical atomic separation distances: 1.6 Å for the Si—O bond, 2.6 Å for O—O and 3.1 Å for Si—Si. These values are in complete agreement with experimental ones.

desirable that each hole in S occupies the largest possible volume in V_{void}, and that the holes in the set intersect each other as little as possible, avoiding in any case that a given hole is completely contained within another. This description is similar to that proposed by Hausdorff [10].

For the purposes of our discussion a hole is then a spherical portion of void space in the system, regardless of its dimension or position. In a restricted sense a hole is equivalent to an interstice, while its radius is smaller than that of the largest particle in the system. As opposed to the analysis by Chan and Elliott [11], this model assumes no structural restriction and thus large gaps in the structure, pores or "defects", are simply accounted for as larger holes.

The procedure for the construction of set S is based on a succession of random positioning holes in V_{void}, in such a way that every new hole will be considered a new element of S if the space it "occupies" is not being largely occupied by some other element in S. The criterion to decide whether a hole should or should not be accepted as an element of S is as follows:

A hole A of radius r_a and centered at P, contains a hole B of radius r_b centered at P', if (see Fig. 3):

(1) B is inside A (that is, $d_{AB} < r_a$, where d_{AB} is the separation between the centres of the holes) and r_b is less than r_a .

Once the containment criterion between holes has been established, the set S is constructed through successive iterations of the following steps:

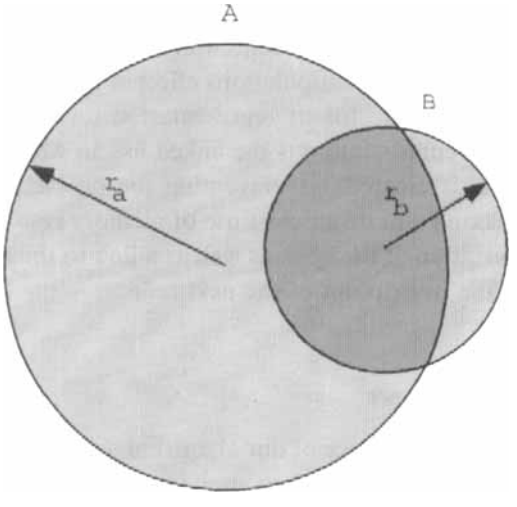

FIGURE 3 Hole containment criterion. Hole B is contained by hole A, and thus discarded from the list.

i) A point P which is contained in V_{void} is randomly obtained.
ii) The radius of the largest possible hole, centered at P, is calculated. The maximum hole radius will be the distance between P and the centre of the nearest particle (i.e., a sphere representing an atom) minus the radius of the particle.
iii) If the resulting hole, centered at P, contains a hole centered at P' (according to (1), above), the latter is discarded from S. If, on the other hand, P' contains the hole centered at P, P is not further considered.
iv) Set S is updated with the hole centered at P.

The above steps are repeated until the maximum number of generated random points is reached.

According to the procedure outlined above, a newly generated hole in a more suitable position will have a larger radius and will better account for the volume previously described by other smaller holes, causing them to be deleted from set S, lowering in the process the cardinality of the set. If the number of random points is large enough, convergence, and thus reproducibility, will eventually be achieved.

Every hole in S touches a particle of the system, and possibly, other holes. It is convenient to stress that the intersection of two holes is not necessarily related to what is known as "door" (see Chan and Elliott [1] and the references therein), and consequently the concept of free volume compartment is not necessarily related to our generic concept of "hole", as the latter arises from probabilistic rather than from deterministic grounds. A free volume compartment will be equivalent to a hole if the former has a spherical shape or else it will be a collection of coalescing holes.

Due to the nature of the manipulations effected on set S, it is convenient to use a dynamic structure for its representation on a computer. A good candidate for such representation is the linked list, in which a new node for each hole in set S is created, circumventing the problems of static array dimensioning, making a more efficient use of memory resources. Each node contains the description of the hole, as well as a link to the next node, which in turn contains the description of the next hole.

3.2. Algorithm Performance

In order to test the performance of our algorithm we chose to analyse a pure amorphous SiO_2 sample, rather than analysing, as is somewhat customary, a dense random packed array of hard spheres. Figure 4 shows a subset of the cavity system corresponding to the vitreous silica matrix of Figure 1 (only

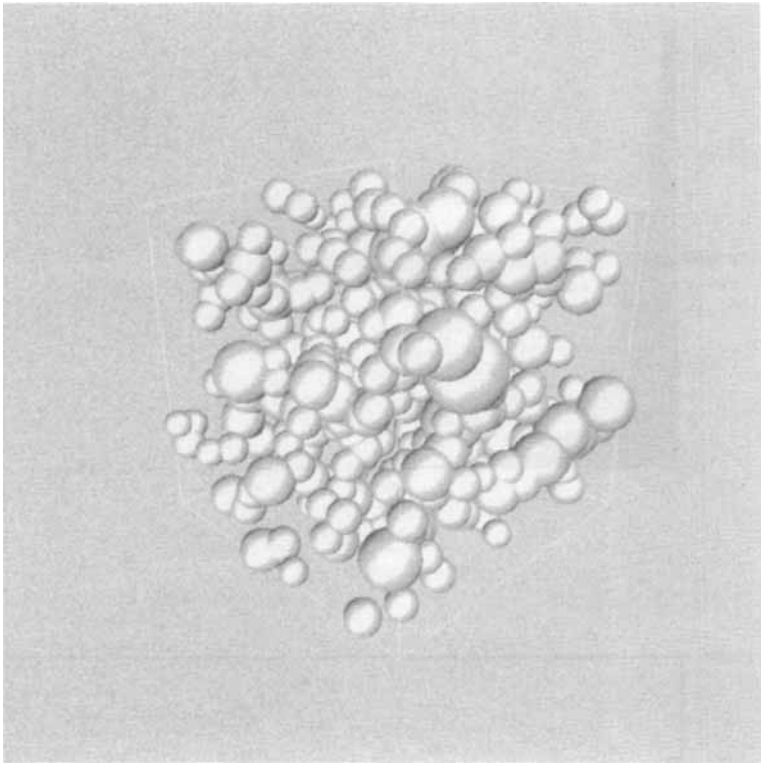

FIGURE 4 Cavity structure corresponding to Figure 1. Holes with a radius smaller than 0.92 Å were not taken into account in the calculation of the cavity set shown. (See Color Plate II).

those holes with radii larger than 0.92 Å are shown). The performance of the hole locator is illustrated in Figure 5a, which represents a hole size histogram for a set of 32,000 holes. Its size distribution seems to be slightly better described by a lorentzian rather than by a gaussian curve. Although small hole sizes possess no physical significance, they do contribute to the allocation of the entire void volume. If r is small enough, however, interstitial space will also be accounted for.

In practice, a set of a few hundred holes suffices to describe the cavity system rather well. On the other hand, for a given choice of minimum r, computational time increases greatly with $1/r$ in order to achieve convergence. It is thus advisable to limit the hole size to the size of the probe to be used (i.e., a given atomic radius).

If the algorithm is run on a physically meaningless, randomly created structure (Fig. 5b), with the same type and number of atoms in the same

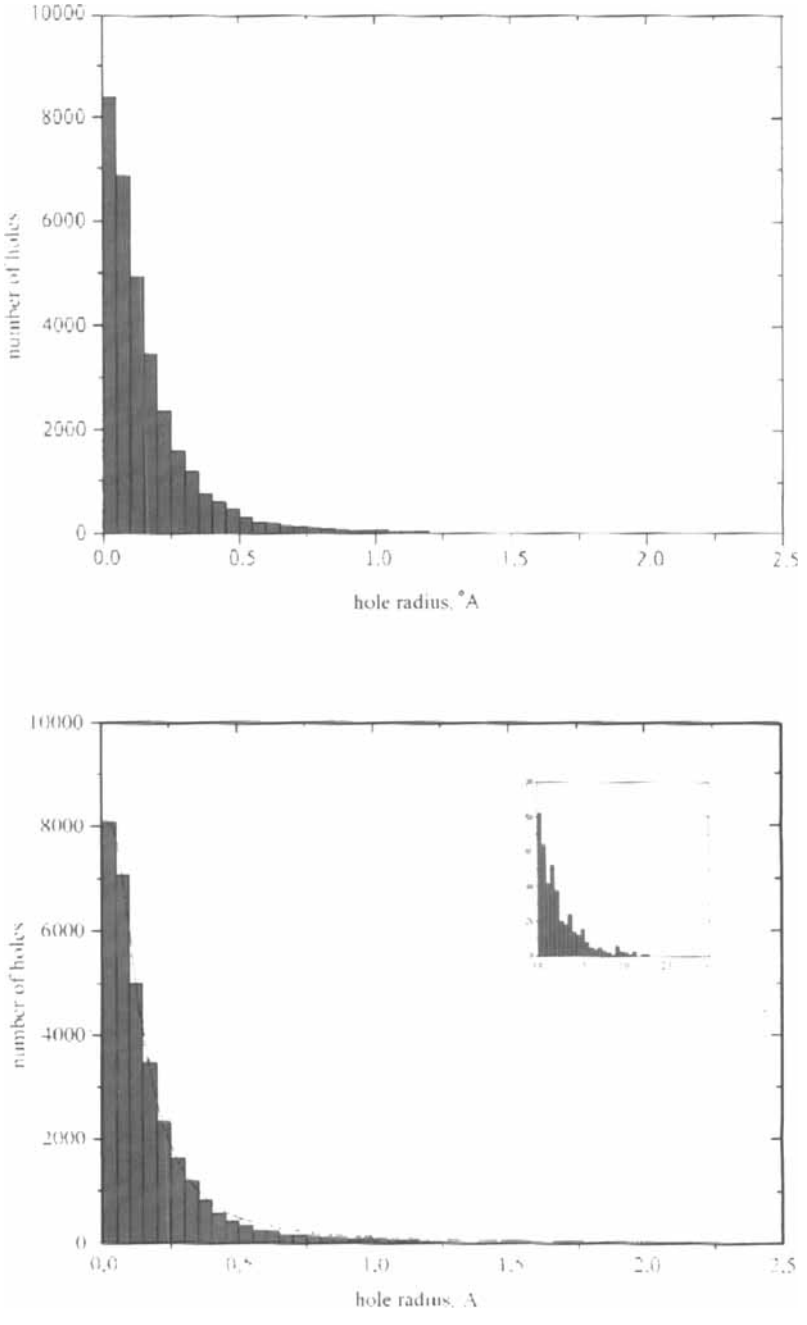

FIGURE 5 Hole size distribution for our amorphous SiO_2 system (Fig. 5a), and for a physically meaningless configuration with the same number and type of atoms randomly relocated in the same volume (Fig. 5b). The distributions are better fit by a lorentzian curve in Figure 5a. The physically relevant part of the hole size spectrum is the right end of Figure 5a (inset), where large holes represent interatomic cavities.

computational box, the 32,000-hole distribution has different values, but it still seems to be lorentzian in shape, which shows that the algorithm is not biased in its overall performance by the structure. In any case, the physically relevant information is located at the right end of the curve, where the system cavities are more appropriately described by a reduced number of larger holes (see inset, Fig. 5a).

The calculation of void volume is carried out using a numerical integration procedure in which the total cell volume is scanned by a small cubic probe. If the space in which the probe is located belongs to a hole, the probe volume is taken as a contribution to the total void volume. The behaviour of the volume fraction allocated as a function of the number of holes found in our structure can be seen in Figure 6a. It is clearly seen that after some 10,000 holes have been located, the total volume accounted for

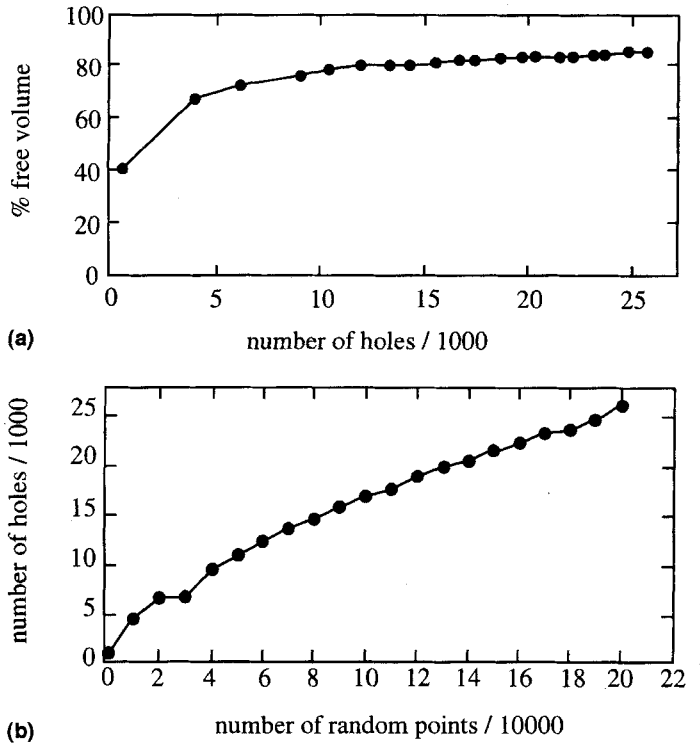

FIGURE 6 Fraction of total cell volume allocated in terms of the number of holes (Fig. 6a), and number of holes located in terms of the number of generated random points (Fig. 6b). The asymptotic behaviour of the volume fraction in terms of the number of holes and the progressive difficulty of locating new holes in the structure are evident.

does not increase drastically. The total volume in the computational cell after locating 25,000 holes is close to 85%, which is fairly good taking into account the random nature of the hole location algorithm. The failure of the algorithm in better allocating the total void volume ultimately reflects the limitations of the random number generator employed.

Figure 6b illustrates the point that it is increasingly difficult to locate a new hole in the structure where no other hole is already present. This has a decisive bearing on execution time, and it also implies that the most important cavities of the structure are quickly found. This is quite relevant in characterising structures with large cavities.

3.3. Connectivity Algorithm

A more complete description of the cavities in a given structure is obtained by analysing the grouping of holes that touch each other into "families" or "cavities". It is necessary to establish a coalescence criterion by which to proceed in analysing hole set S, as follows:

Given any two holes A and B, the distance d_{AB}, between their centres must be such that:

$$d_{AB} \leq r_a + r_b + \varepsilon,$$

where r_a and r_b are radii of hole A and B respectively, and ε is the tolerance (see below). By using the above criterion it is possible to identify a hole family by recursively writing into a list a hole, all its neighbours, and all the neighbours of their neighbours, etc., until no more holes can be included in the list.

The connectivity of the family will be the sum of the distances between coalescing holes. This quantity represents the path a probe of a given size can traverse without abandoning the same cavity. It is to be noted that the applicability to the physical world of the concept of connectivity in the sense used here is rather limited, mainly because we forgo the analysis of the electrical environment within the cavities and their fluctuating nature [12, 13]. Nevertheless, useful information can be derived from this datum (see below). Figure 7 shows the total connectivity (the sum of the connectivities of all families) in terms of the maximum number of random points generated by the hole locator for a pure amorphous SiO_2 sample. The probe size was in our case 0.92 Å (the radius of a Li^+ ion according to [14]. In a future paper we will report on our findings in the system $xLi_2O(1-x)SiO_2$). Note that the connectivity levels off when the number of random points is

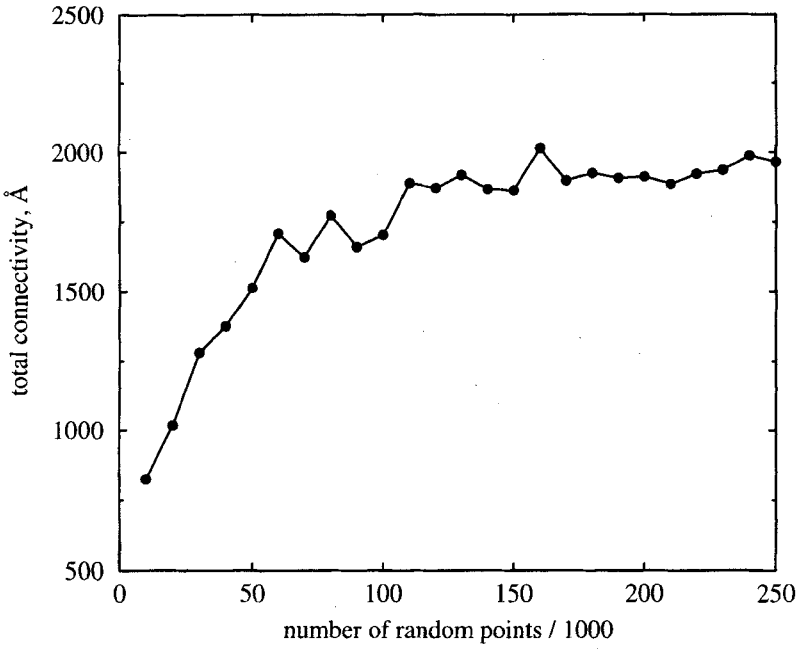

FIGURE 7 Total connectivity *versus* number of generated random points. It can be seen that the connectivity approaches an asymptotic value after an initial sharp rise. In order to save computing time it is advisable to choose an intermediate value of the number of random points.

around 125,000. This is then a good choice if we want to obtain a reasonable accuracy with the least possible processing time. Although this levelling off occurs at a much greater number of random points than it occurs for the volume calculation shown in Figure 6a, this is due exclusively to the constraint we imposed that the connectivity must be described by holes of radii larger than 0.92 Å.

As outlined above, if the hole locating algorithm were to run with a very large number of random points, the hole centres would eventually converge to their optimum value, at the expense of processing time growing non-linearly with the number of points. In order to obtain accurate overall values in short times it is convenient to give the coalescence criterion some latitude, by means of parameter ε. The influence of ε on the average connectivity can be seen in Figure 8, where the average connectivity represents the total connectivity divided by the number of families present. Single, isolated holes are not counted as families.

If two families are separated by a distance equal to or less than ε, they can be regarded as a single family, if the gap ε is not large enough to cause them

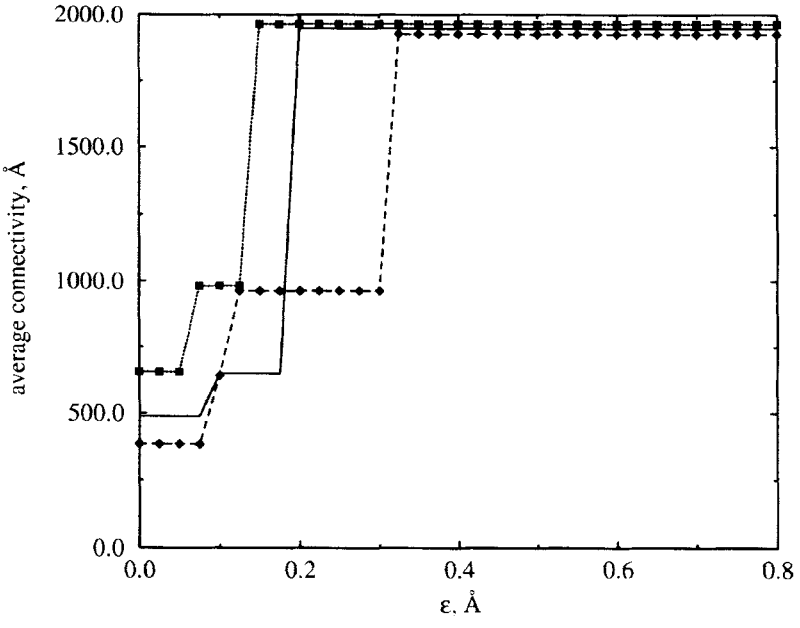

FIGURE 8 Influence of latitude parameter, ε, on average connectivity. It can be seen that the average connectivity value, the total connectivity divided by the number of families, increases stepwise upto a certain value of ε, around 0.2, where the average connectivity represents the total connectivity value, as all families coalesce into a single one. In this particular case the entire cavity system seems to be comprised of only one large, multi-branched cavity.

to bridge across the smallest atom in the system. The right choice of ε will depend strongly on the system, and will guarantee more consistent results.

4. PERCOLATION ANALYSIS OF a-SiO_2

In the former sections we have shown results that pertain mainly to the algorithm rather than to the simulated system. We will show here that this algorithm can prove useful in determining important structural features of vitreous silica, namely its percolation behaviour and its number of rare-gas solubility sites.

As was previously outlined, if a chemical species is to dissolve in a solid matrix, its ability to penetrate into the matrix will be determined, in a simplified view, by the size of the dissolving species and also by the size and number of the cavities in the matrix. Once this is known, a percolation graph such as those in [1, 11, 15, 16] can be made, in which the total volume of compartments that can accommodate a probe of given radius are plotted

against its radius. In Figure 9 we present an equivalent graph for our amorphous silica system, in which we plot the normalised volume allocated by holes of radii greater than or equal to that indicated in the x-axis. Without regard to the different methodologies there is a certain similarity in the shape of Figure 9 with those in refs. [1, 11, 16]. The physical implication of this curve is that a probe of a given size will be able to travel through greater zones in V_{void} (if the constituent parts of them are connected) as the probe size decreases. It is therefore necessary to establish the radius of the probe for which there will be no structural hindrance for it to travel freely across the bulk. This cannot be clearly determined from Figure 9. Thus, the usual term "percolation graph" is somewhat of a misnomer for it.

The concept of "family" described in Section 3.3 can be of use in determining the radius alluded to above, known as the *percolation radius*. If a family is a subset S' of S, in which each hole has a neighbouring hole that touches it, and N is the number of families, then the smaller the holes, the larger the cardinality of S', and also, the lower the value of N. In the lower

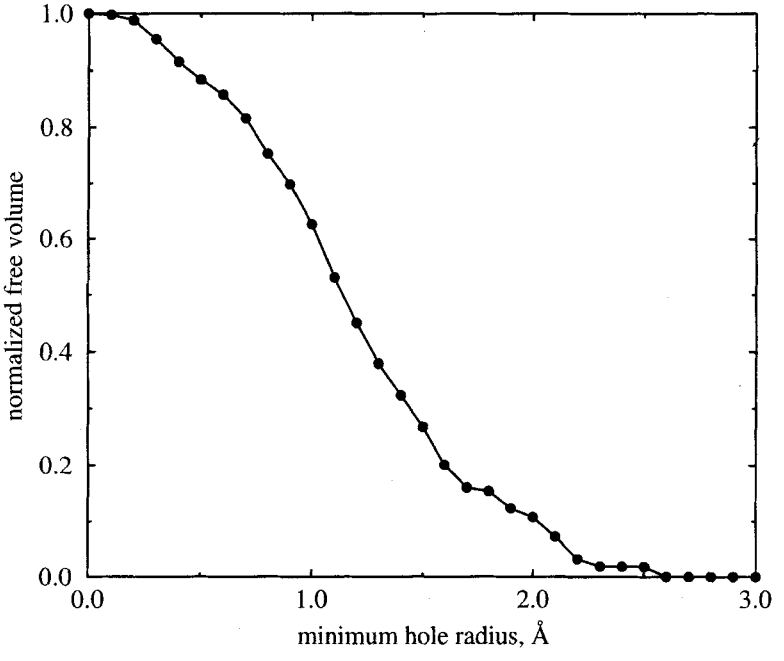

FIGURE 9 'Normalised volume allocated by holes of radii greater than or equal to that indicated by x-axis. A probe particle will be able to travel through greater zones in V_{void} as the probe size decreases.

limit, $N = 1$ and $S' = S$, and its cardinality is maximum *with respect to that of* S. Note that this is not in opposition to the desired property of minimum *overall* cardinality set forth in section 3.2. In the upper limit, on the other hand, bigger holes will be isolated in the structure and will not form families, which implies that $N = 0$ and the cardinality of S is minimum.

Figure 10 responds to what we believe is more properly denominated "percolation graph". It shows the behaviour of N with the minimum hole radius. As expected, there is a region in which the entire cavity system is comprised of a single family. Fragmentation begins at about 0.7 Å, which corresponds to the maximum radius a probe could have if it were to travel freely throughout the silica matrix. This is known as the percolation radius, r_p. It is interesting to note that, using geometric arguments, Chan and Elliott [11] arrive at the conclusion that the percolation radius of vitreous silica

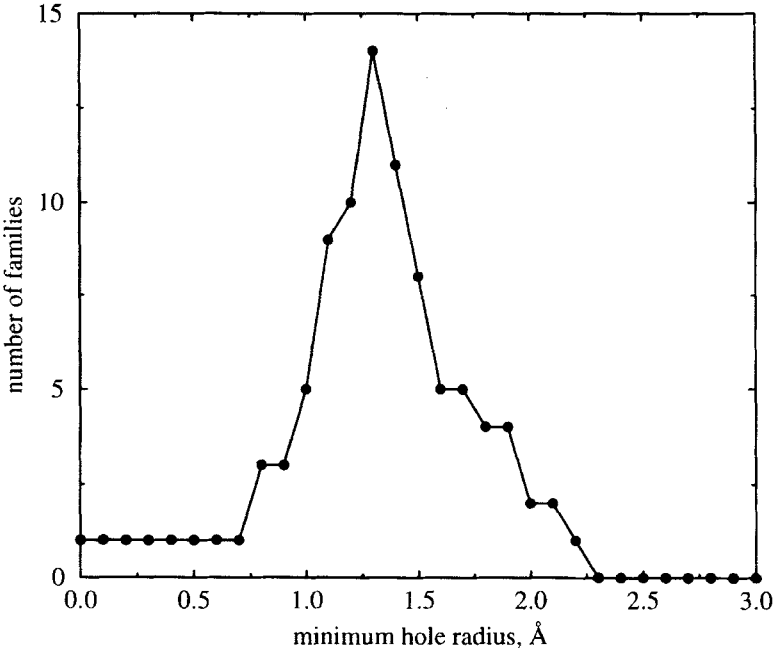

FIGURE 10 Number of families (denoted as N in the text) *versus* minimum hole radius. Note that for smaller probe sizes there is a single family of holes -a single cavity, in our context- where a probe with a radius smaller than or equal to that indicated by x-axis can travel freely throughout the structure. At about 0.7 Å there begin to appear obstructions in the path of the probe. This value is the *percolation radius*, r_p, of the amorphous silica. For larger minimum hole radii a maximum number of families will be reached, until the families begin to disappear, remaining only large, isolated holes (which are not counted as families).

must be 0.60 R_o, where R_o is the oxygen radius. Using Shannon and Prewitt's [14] oxygen radius of 1.21 Å, in which we based our molecular dynamics calculations, $r_p = 0.60 * 1.21 = 0.726$ Å, in agreement with our result (although those authors obtain a larger value by using Bondi's Van der Waals radius for the oxygen). We can now go back to Figure 9 and interpolate the fraction of volume available to the percolating atom to obtain the value of 0.189, which is not far from 1/3, reported in [11] (although for the percentage of available sites, which is closely related to the available volume fraction).

It must be stressed that the small percolation radius of the vitreous silica structure precludes percolation studies with gas solubility techniques. Nevertheless, it is possible to estimate the number of solubility sites per cubic centimetre in our structure, *Ns*, by counting the number of holes large enough to accommodate a probe, or "penetrant", of a given size, namely the Van der Waals radii of helium and neon atoms, 1.8 Å and 1.6 Å, respectively.

If we take into account that there are $(21.4003 \times 10^{-8})^{-3} = 1.02 * 10^{20}$ of our computational cells per cubic centimetre, multiplying the number of holes of suitable size per computational cell, obtained by averaging out the results of 20 runs of the hole locator, our estimate for *Ns* is $20.45 * 1.02 \times 10^{20} = 2.09 \times 10^{21}$ solubility sites per cubic centimetre for He, very close to the experimental value reported by Shackleford (see [11]), 2.3×10^{21}, and $35.65 * 1.02 \times 10^{20} = 3.64 \times 10^{21}$ solubility sites per cubic centimetre for Ne, not too far from Shackleford's experimental value of 1.3×10^{21}.

5. CONCLUSIONS

We have presented a simple and powerful "Swiss-cheese" cavity locating algorithm suitable to be applied to, but not limited to amorphous systems. The algorithm recursively optimizes the void volume allocation while minimizing the hole count. By defining a "family" as a set of coalescing holes we were able to locate the onset of percolation in a simulated silica structure with periodic boundary conditions, at about 0.7 Å. On these grounds we suggest an alternative form of a percolation graph. We have also made a good approximation to the experimental value of the number of solubility sites for rare gases in silica.

In this article we have tried to illustrate the point that a good deal of useful information, which is not fully accessible to existing experimental methods, can be derived from simulations along the lines of this work.

Acknowledgements

This research was supported by the Commission of the European Communities under research grant CI1*-CT92-0016, and in part by Cray Research, Inc., under supercomputing grant UNAM-CRAY, DGAPASC-005496. We gratefully acknowledge Raúl Segura for his help on an earlier version of the C-program code of the hole locator, Selene Salas for her help with the figures, as well as Pedro Bosch and Jorge Sánchez for their participation in the critical discussion of the contents.

References

[1] Chan, S. L. and Elliott, S. R. (1990). *J. Non-Cryst. Solids*, **124**, 22.
[2] Bernal, J. D. (1964). *Proc. R. Soc. London*, **A280**, 299.
[3] Lançon, F., Billiard, L. and Chamberod, A. (1984). *J. Phys.*, **F14**, 579.
[4] Whittaker, E. J. W. (1978). *J. Non-Cryst. Solids*, **28**, 293.
[5] Ahmadzadeh, M. and Cantor, B. (1981). *J. Non-Cryst. Solids*, **43**, 189.
[6] Frost, H. J. (1982). *Acta Metall.*, **30**, 889.
[7] Trohalaki, S., DeBolt, L. C., Mark, J. E. and Frisch, H. L. (1990). *Macromolecules*, **23**, 813.
[8] Alavi, A., Alvarez, L. J., Elliott, S. R. and McDonald, I. R. (1992). *Phil. Mag. B.*, **65**, 489.
[9] Mozzi, R. L. and Warren, B. E. (1969). *J. Appl. Cryst.*, **2**, 164.
[10] Hausdorff, F. (1919). *Math. Ann.*, **79**, 157.
[11] Chan, S. L. and Elliott, S. R. (1991). *Phys. Rev. B.*, **43**(5), 4423.
[12] Takeuchi, H. (1990). *J. Chem. Phys.*, **93**(1), 2063.
[13] Sok, R. M. and Berendsen, H. J. C. (1992). *J. Chem. Phys.*, **96**(6), 4699.
[14] Shannon, R. D. and Prewitt, C. T. (1965). *Acta Crystallogr.*, **B25**, 725. *ibid.*, **B26**, 1046 (1970).
[15] Vogl, O., Xi, F. and Vass, F. (1989). *Macromolecules*, **22**(12), 4660.
[16] Greenfield, M. N. and Theodorou, D. N. (1993). *Macromolecules*, **26**, 5461.